LSST DESC Notes

LSST Catalog-level Realization of Gravitationally-lensed Quasars

Jenny Kim,[1] Phil Marshall,[1,2] Mike Baumer,[1,2] Steve Kahn,[1,2] and Rahul Biswas[3]
(LSST Dark Energy Science Collaboration)

[1] *Kavli Institute for Particle Astrophysics & Cosmology, P. O. Box 2450, Stanford University, Stanford, CA 94305, USA*
[2] *SLAC National Accelerator Laboratory, Menlo Park, CA 94025, USA*
[3] *University of Washington*

The scale of the LSST dataset will be such that, when considering the problem of finding lensed quasars, we should anticipate extracting as much information out of the the catalogs as possible before turning to the pixel-level data. In this work we explore the use of simple, low multiplicity Gaussian mixture models for realizing gravitational lens systems in LSST catalog space, to enable both large-scale sample simulation and direct model inference.

This LSST DESC Note was generated on: March 20, 2018

1. Introduction

The Large Synoptic Survey Telescope (LSST), a wide-field survey telescope with the diameter of 8.4m, will start running in Chile in 2020 Ivezic (2008). This telescope has a 3.5 deg of field of view, would cover around 30000 *deg*^{2} in the sky, and uses u, g, r, i, z, and y filters LSST Science Collaboration (2009). The telescope will give an extensive amount of astronomical data that could be used for the study of Solar System, Extragalactic structures, near-Earth asteroids, radiant radio sources, Dark Matter, and Dark Energy LSST Science Collaboration (2009).

LSST Dark Energy Science Collaboration (DESC) also anticipate to detect around 8000 strongly lensed systems that will provide useful information such as cosmological time delay or lens mass distribution LSST Dark Energy Science Collaboration (2012) Treu & Marshall (2016) LSST Science Collaboration (2017). Time delay could be used to infer cosmological parameters Auger et al. (2010) which describes the state of the universe.

In order to perform such research, finding the lensed system among the enormous set of data is crucial. However, LSST is also expected to produce 80 terabytes of data each night LSST Science Collaboration (2009). Considering the amount of the data that LSST will produce, pixel-level searching with images(Gavazzi et al. (2014)) may be impossible. In order to solve the problem, we propose the lens classification with catalog-level searching with machine learning techniques (SLRealizer).

The attempt to use Machine Learning to detect lensed system is not a completely new idea. (Petrillo et al. 2017) suggests that morphological classification of the lensed system using the Convolutional Neural Network(CNN) could be effective. (Pourrahmani et al. 2017) has developed 'lensextractor' that uses convolution neural network to train and test the software to detect the lensed system.

The 'SL Realizer' project largely consists of two major parts: finding the useful feature sets to classify the lensed systems from other objects and classifying the lensed systems with different machine learning algorithms.

2. Method

2.1. Preparation of Data

Twinkles, a simulated LSST sky with observed with six filters for ten years, provided the ten years of mock observation history. We also had OM10 mock lensed systems Treu & Marshall (2016).

We assumed that OM10 mock lensed systems are composed of point-like sources. This means that the size of the galaxies as well as the quasar images had the effective radius of zero.

obsHistID	expMJD	filter	FWHMeff	fiveSigmaDepth
183767	59823.286523	g	1.093153	24.377204
183811	59823.307264	g	1.23193	24.289872
184047	59823.418685	z	0.908511	21.923566
185595	59825.256044	r	0.949096	24.128617
185736	59825.325979	g	1.242407	24.316968
185785	59825.352519	g	1.139232	24.436879
187493	59827.2603	z	0.807941	22.896684
187525	59827.278039	z	0.789221	22.990253
187546	59827.287816	z	0.748829	23.078407
187589	59827.307705	z	0.78313	23.152559
187603	59827.314787	z	0.737639	23.278169
188992	59831.282065	y	0.864951	21.637001
188998	59831.284749	y	0.86527	21.638293
189408	59832.286563	y	0.927227	21.565914
189410	59832.287459	y	0.892628	21.607713
189438	59832.300037	y	0.901127	21.603858
190235	59835.229203	y	0.687516	21.848489
190247	59835.234574	y	0.697389	21.839287
190261	59835.240838	y	0.682609	21.869248
190486	59835.342307	y	0.740154	21.831827
190506	59835.352406	y	0.726127	21.853582
191253	59836.27921	z	0.805327	22.48682
191280	59836.291765	z	0.89064	22.393466
191299	59836.300643	z	0.877464	22.419594
191340	59836.319672	z	0.842551	22.481365
192895	59839.212084	r	0.87897	23.996169
193130	59839.325615	r	0.910452	24.026352
193170	59839.34463	r	0.72798	24.269137
195529	59842.194696	r	0.969729	24.064754
196438	59843.19904	i	0.959816	23.441221
196476	59843.216405	i	0.8201	23.655955
196570	59843.258667	i	0.909227	23.621382
196611	59843.280976	i	0.745115	23.86419
197356	59844.223991	r	0.830065	24.326122
197394	59844.241759	r	0.854513	24.329096
199504	59849.203519	r	1.224899	23.888403
199540	59849.219946	r	1.173648	23.969609
200152	59850.223152	i	1.057096	23.432202
200184	59850.241578	i	0.977688	23.543202
200705	59851.196667	u	1.300213	22.885441

In order to save some computation time, we queried the first three years of the observation which yields 263 observation epochs. We also selected LSST-like OM10 mock lensed systems by querying with magnitude cut of 22.5.

3. Data Preparation

3.1. Toy Source Catalog

Using the data from subsection 2.1, we were able to make an each entry of catalog describing how each lensed system would look like on a particular night. While doing this, we assumed that all the sources in the lensed system have Gaussian point spread functions. Also, we realized the systems with a null-deblender, meaning that we assumed that all the lensed images and the lens were observed as one big source.

In order to do so, we used Galsim package in Python. For each lensed system, we drew a Gaussian that has an effective radius of a galaxy as well as adding the rotation angle and shears to the values. We also drew the Gaussians that have an effective radius of zero in the position for the quasar images. Then, we convolved the Gaussians with the Gaussian point spread functions. After then, we added all the convolved Gaussian onto the two-dimensional grid that has the same degree-to-pixel ratio (0.2 arcseconds per pixels) as LSST, realizing the total sum as one Gaussian. After the realization, we could get ellipticity, zeroth moment, the first moment, and the second moment per one big convolved Gaussian.

The toy catalog is in subsection 3.1.

3.2. Toy Object Catalog

After generating the source catalog, we computed the object table whose entree describes average properties of each lensed system per filter. In order to do so, we queried each lensed system in the source catalog. Then, for each lensed system, we computed the average properties for each filter.

The toy catalog is in subsection 4.2.

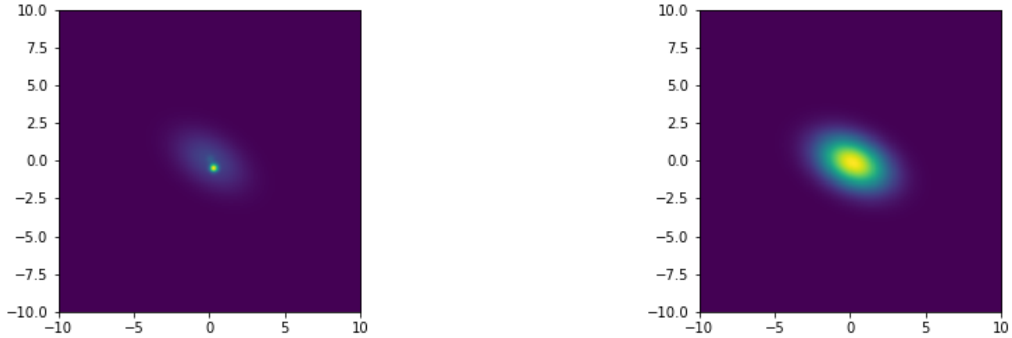

Figure 1. Example null-deblending in OM10 lens system 4898214. Image axes show offsets from the center of the lensed system in arcsec. Left: Realization of the lens system with zero-width PSF. The brightest source is the lensing galaxy, and there are two dimmer quasar images near the galaxy. There is only one quasar image that is obvious; this makes the blended object appear elliptical. Right: Realization of the lens system with realistic PSF. All the components of the system appear blended together. The color bar shows rescaled surface brightness: overall, flux is conserved between the two images.

3.3. Feature Selection

For now, we focused on classifying the lensed systems from the SDSS galaxies. We expect the lensed images to appear near the bright, massive galaxies. Thus, if we can differentiate the galaxies with lensed images with the galaxies without them, it would be really helpful.

We expect that the quasar images will be brighter in the shorter wavelength filters. The galaxies will be brighter in the longer wavelength filters. Thus, when we observe a lensed system through a u filter (the shortest wavelength filter that OM10 has), we will see the more stretched object because of the contribution from the quasar images. However, in the z band, we will see a round object because of the contribution from the lens. By comparing the features in the u filter and the z filter, we will thus be able to see bigger changes in the properties for the lensed systems than SDSS galaxies.

The features that we could get from the object table is changes in the first moment along the x-axis (reference to the r filter), changes in the first moment along the y-axis (reference to the r filter), changes in the position (reference to the r filter), ellipticities, rotation angles, fluxes, and sizes.

The catalog of SDSS galaxies also provides the same features. Magnitude systems are the same in both SDSS and OM10, and the units are scaled to be the same. However, the only difference was in the sizes. SDSS's definition of size was I_{xx} + I_{yy}. Galsim calculates the size of OM10 systems by calculating the determinant of the second moment(M $= I_{xx}$ * I_{yy} - I_{xy} * I_{xy}) and applying the fourth root on it ($\sqrt[4]{M}$). In order to solve the problem by scaling the SDSS sizes, we multiplied the power of pixel-to-arcsec ratio to change the unit to arcseconds, multiplied two to convert the half size to the full size, and applied the square root to the value to get a right dimension.

Using these values, we computed various additional features. We plotted SDSS galaxies and OM10 lensed systems onto the corner plot subsection 3.3, and chose the features that differentiated OM10 lensed systems from SDSS galaxies the most.

3.4. Classification

We have 2323 OM10 lensed systems and 16000 SDSS galaxies. In order to make the balanced test data set, we randomly selected 2323 SDSS galaxies. We mixed the order of those two samples so that there will be a roughly same number of each OM10 and SDSS samples in both the test and the training data. Then, using the scikit train_test_split method, we selected 75$\%$ of the data to be the training set and performed the test on the remaining 25$\%$.

According to the scikit's choosing the right estimator, we were able to choose three different algorithms for the classification purposes. We did have more than 50 samples, we were predicting a category, we did have a labeled data, and we had less than 100K samples in a text data. This yields Linear SVC, KNeighbors Classifier, and Ensemble classifiers such as Random Forest.

Detailed results are in subsection 4.4.

4. Results

4.1. Toy Source Catalog

lensid	MJD	filter	RA	RA_err	DEC	DEC_err	x	x_com_err	y	y_com_err	flux	flux_err	size	size_err	e1	e2	e	phi	psf_sigma	sky
710960	59823.286523	g	0	0	0	0	2.1350	0	1.2151	0	21.9127	0.03549	1.4501	0	0.2386	0.3360	0.4121	0.4766	1.093153	24.377204
17432684	59823.286523	g	0	0	0	0	0.1226	0	0.7593	0	18.2072	0.03549	1.1802	0	-0.0550	-0.004712	0.05525	0.04270	1.093153	24.377204
50310149	59823.286523	g	0	0	0	0	0.2527	0	0.4665	0	5.9831	0.03549	1.2253	0	-0.05931	0.02588	0.06471	-0.2057	1.093153	24.377204
52812164	59823.286523	g	0	0	0	0	0.3874	0	-0.3413	0	6.2727	0.03549	1.2102	0	-0.03114	-0.05654	0.06455	0.5336	1.093153	24.377204

Table 2. Few sample entrees of the toy source catalog. The full toy object catalog can be viewed here

The above is the toy source catalog that we generated. For now, we haven't added error terms and calculated the positions (RA and DEC).

4.2. Toy Object Catalog

Table 3 is the toy object catalog that we generated.

4.3. Feature Selection

Full corner plots can be viewed in the SLRealizer's GitHub repository's notebook folder.

As mentioned in subsection 3.3, we thought comparing features between u and z filter will be discriminatory. We chose six main features that we thought would change dramatically between the filters for OM10 lenses – sizes, ellipticities (e), rotation angles of galaxies (ϕ), magnitudes, positions(Δ x), and the angle between ellipticity vector and the rotation vector ($\omega = \frac{e\cdot\phi}{|e||\phi|}$).

Here, the centroid of the yellow points(SDSS galaxies) and the purple points(OM10 systems) differed the most for size. Still, we could quantify the importance of the features by putting all the data into the Random Forest Algorithms. The results were as follows.

lensid	u_flux	u_x	u_y	u_size	u_flux_err	u_x_com_err	u_y_com_err	u_size_err	u_e1
710960.0	37.0846	2.2817	1.2996	1.4151	0.2511	0.0	0.0	0.0	0.1399
17432684.0	26.7018	0.1211	0.7633	0.971	0.2516	0.0	0.0	0.0	-0.0968

g_flux	g_x	g_y	g_size	g_flux_err	g_x_com_err	g_y_com_err	g_size_err	g_e1	g_e2	g_e
19.9485	2.1555	1.2328	1.4608	0.1244	0.0	0.0	0.0	0.1967	0.2768	0.3
17.5991	0.1221	0.7518	1.2413	0.1244	0.0	0.0	0.0	-0.0532	-0.0045	0.0

r_flux	r_x	r_y	r_size	r_flux_err	r_x_com_err	r_y_com_err	r_size_err	r_e1	r_e2	r_e
31.0886	2.27	1.2928	1.2608	0.0923	0.0	0.0	0.0	0.1693	0.2395	0.29
25.2258	0.1215	0.7617	0.9958	0.0923	0.0	0.0	0.0	-0.0867	-0.0078	0.08

i_flux	i_x	i_y	i_size	i_flux_err	i_x_com_err	i_y_com_err	i_size_err	i_e1	i_e2	i_e
26.2547	2.3012	1.3075	1.2154	0.0433	0.0	0.0	0.0	0.1521	0.2146	0.263
22.747	0.1217	0.7612	1.0063	0.0433	0.0	0.0	0.0	-0.0813	-0.0071	0.081

z_flux	z_x	z_y	z_size	z_flux_err	z_x_com_err	z_y_com_err	z_size_err	z_e1	z_e2	z_e
19.7955	2.264	1.2879	1.2545	0.0322	0.0	0.0	0.0	0.1595	0.2247	0.2
18.0387	0.1216	0.7587	1.0622	0.0315	0.0	0.0	0.0	-0.0751	-0.0064	0.0

Table 3. Few sample enrees of the toy object catalog. The full toy object catalog can be viewed here

4.4. Classification

As mentioned in subsection 3.4, we used three different algorithms: linear SVC, KNeighbors (Nearest Neighbors), and Random Forest. Figure 6 is the results that we got for each algorithm.

Random forest showed the best performance among the three different algorithms. If we look into the top left corner where all the curves are overlapped, we can see this more obviously. The best classifiers were Random Forest, and the more the number of estimators were, the better the algorithm performed. For the best algorithm, we were able to achieve 98% of the true positive rate(TPR) and 0.04% of the false positive rate(FPR).

5. Conclusions

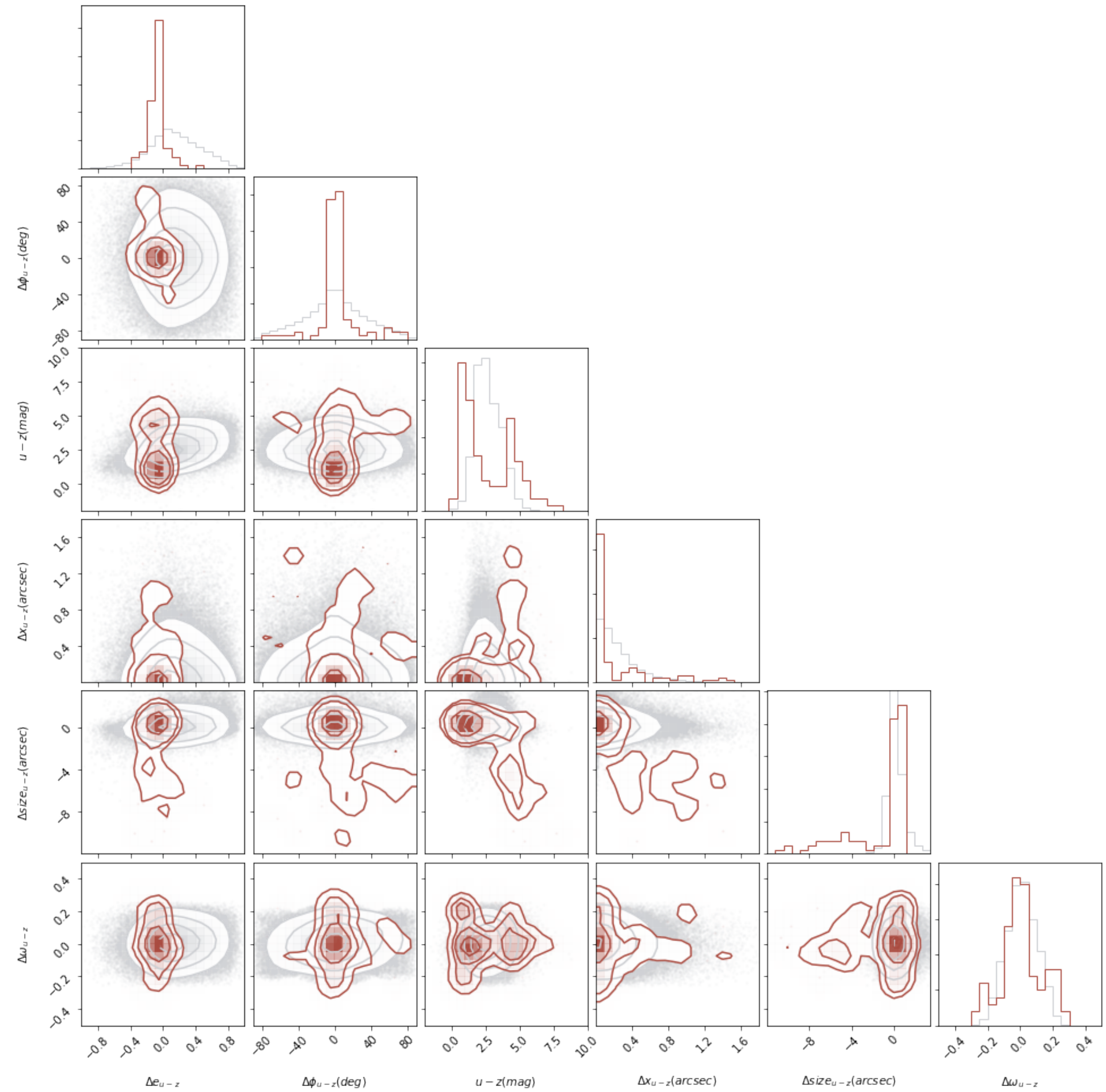

Figure 2. The cornerplot with six features.

The results suggest that random forest algorithms would be able to differentiate lensed systems from galaxies. Still, even though we have high accuracy, because we expect to have much more non-lensed systems than the lensed systems, we will have more contaminants in the truly-classified lensed systems than the actual lensed systems. For instance, we expect to find 10,000 times more non-lensed systems than the lensed ones. Thus, with 98% of the TPR and 0.042% of the FPR, we will have 430 contaminants per truly classified lensed systems. Thus, it would also be helpful to have a more rigorous

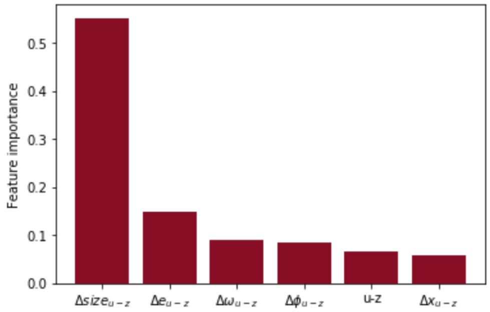

Figure 3. Feature importance calculated with the Random Forest algorithm.

model that actually fits physical models to the systems after rejecting all the non lensed-systems using SLRealizer.

In addition, we only compared the features between OM10 lensed systems and SDSS galaxies. It will also be useful to overlap star-star pairs, star-galaxy pairs, quasar-quasar pairs, or quasar-galaxy pairs to see how different the other samples could be from the lensed system.

There are few ways to further improve the classifiers. If we could implement the working deblender that resembles LSSTs deblender, that will increase the performance of the classifiers. We could also add more features such as time-variabilities of quasar images. While making the source and the object catalog, rather than giving equal weights to all the observations, we could weight by how good the seeing was for each night.

In addition, while studying cosmology, gravitationally lensed systems with four images (quads) are generally more useful than the systems with two images (doubles). Thus, comparing how many quads were classified as true out of the testing samples quads should also give useful statistics.

Acknowledgments

This research was partially supported by Stanford Physics Departments' summer research grant. I would like to thank Prof. Kahn, Dr. Marshall, and Mike Baumer for their helpful advice and insights. We would also like to thank Rahul Biswas and LSST DESC collaboration for providing their expertise and guidance for the paper.

[bt]0.48

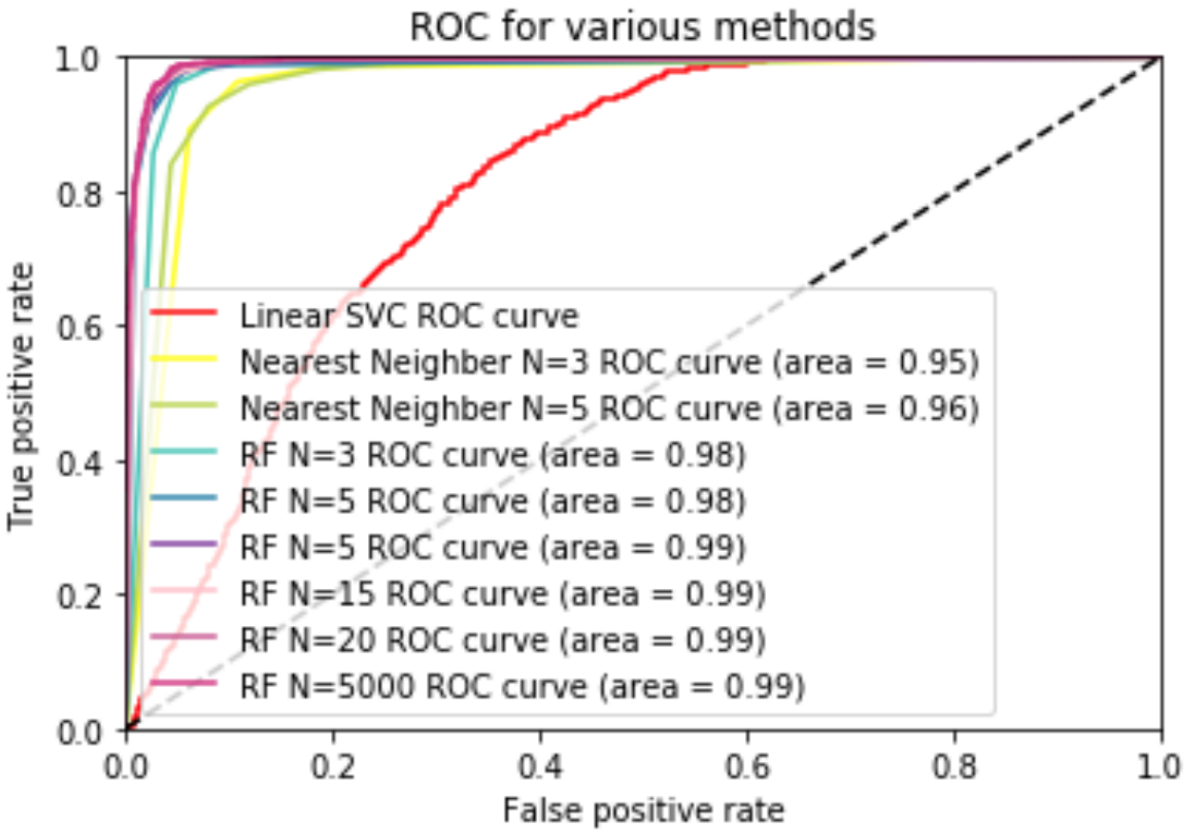

Figure 4. ROC curve for each algorithm

[bt]0.48

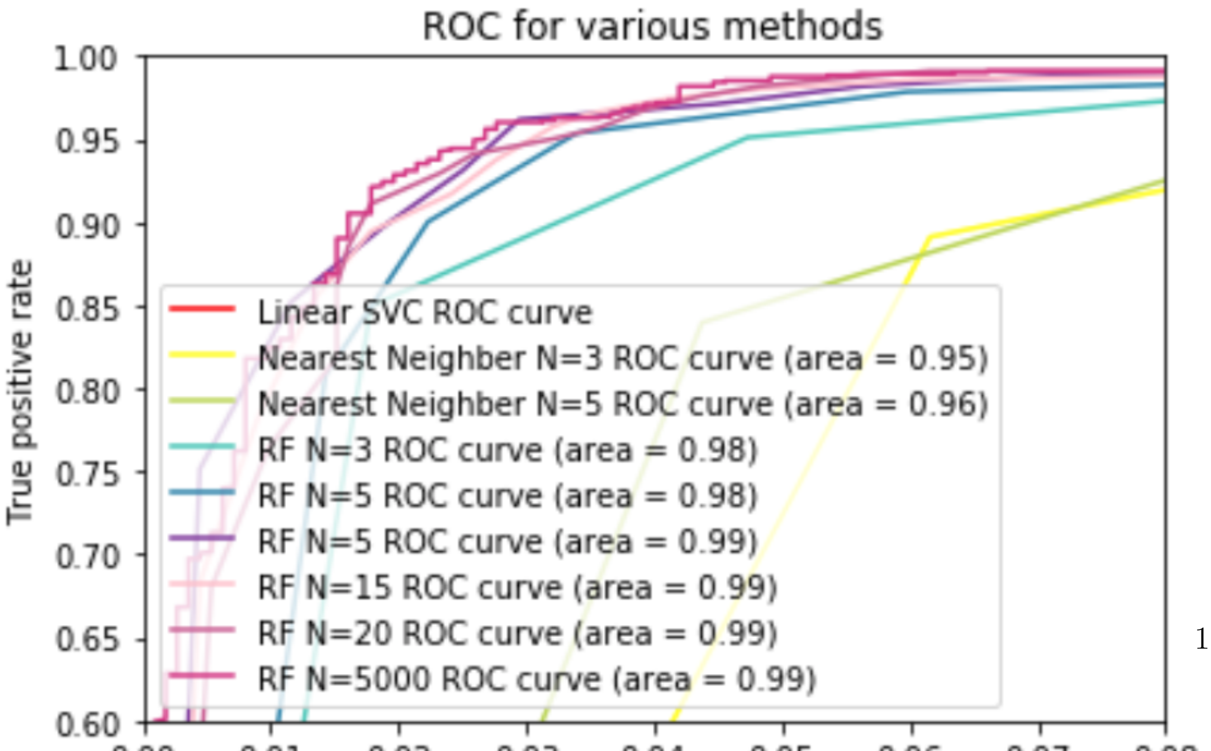

Author contributions are listed below.
Jenny Kim: Led algorithm and code development, wrote paper.
Phil Marshall: Initiated project, advised on motivation, model construction and testing.
Mike Baumer: Advised on LSST data characteristics, model construction and testing.
Steve Kahn: Advised on LSST data characteristics, model construction and testing.
Rahul Biswas: Advised on LSST observing cadence, catalog characteristics, error model.

References

Auger, M. W., Treu, T., Bolton, A. S., et al. 2010, ApJ, 724, 511

Gavazzi, R., Marshall, P. J., Treu, T., & Sonnenfeld, A. 2014, ApJ, 785, 144

Ivezic, Z. 2008, ArXiv e-prints, arXiv:0805.2366

LSST Dark Energy Science Collaboration. 2012, ArXiv e-prints, arXiv:1211.0310

LSST Science Collaboration. 2009, ArXiv e-prints, arXiv:0912.0201

—. 2017, https://github.com/LSSTDESC/Twinkles

Petrillo, C. E., Tortora, C., Chatterjee, S., et al. 2017, ArXiv e-prints, arXiv:1702.07675

Pourrahmani, M., Nayyeri, H., & Cooray, A. 2017, ArXiv e-prints, arXiv:1705.05857

Treu, T., & Marshall, P. J. 2016, A&A Reviews, 24, 11